ROLES OF ADSORPTION POTENTIAL AND SURFACE FREE ENERGY ON PURE CH_4 AND CO_2 ADSORPTION UNDER DIFFERENT TEMPERATURES

by

Tong-Qiang XIA[a,b,c] *, Jing-Yu MENG[a], You-Pai WANG[a], Jian-Hong KANG[a], Hong-Yun REN[a]

[a]Key Laboratory of Coal Resources and Safe Mining, China University of Mining and Technology, Xuzhou 221008, China

[b] Hebei State Key Laboratory of Mine Disaster Prevention，North China Institute of Science and Technology，Beijing 101601，China

[c] College of Mining Engineering, Liaoning Technical University, Fuxin, Liaoning 123000, China

To fill the knowledge of adsorption characteristics of CH_4 and CO_2 associated with equilibrium and thermodynamics, adsorption equilibrium tests of pure gas on a coal were conducted under the different temperatures (35^oC, 50^oC and 65^oC) by the static volumetric method. The equilibrium data were well matched by the SLD-PR model. The influence of some significant factors including temperature, pressure, adsorption potential and surface free energy on gas adsorption capacity were discussed. The results showed that the higher temperature (gas pressure) corresponds to the smaller (larger) adsorption capacity; the larger adsorption potential is, the smaller adsorption capacity is. Taking CH_4 as adsorbent, the modified Langmuir equation can well match the SLD-PR model. However, when the adsorption medium is CO_2, modified Freundlich equation is better. Using the two modified equations, we study further the relationship among the variation of surface free energy, its reduction rate and gas adsorption capacity. It can be concluded the larger the gas adsorption capacity is, the greater the reduction of surface free energy is, and the smaller the reduction rate of surface free energy is.

Key words: *gas adsorption, SLD-RP model, adsorption potential, surface free energy*

Introduction

Advances in the understanding of coal–gas adsorption characteristics have changed the manner in which we enhance coalbed methane (ECBM) recovery through other gas injection into the coalbed (eg. pure/a mixture of CO_2 and N_2)[1-3]. They are different ECBM mechanisms between with CO_2 and N_2 as injectants. When CO_2 is injected, CH_4 is displaced from coal because of the stronger adsorption of CO_2. While N_2 as injectant, CH_4 is desorbed from coal due to the reduction of the partial

* Corresponding author Tong-Qiang XIA; E-mail: tq.xia@cumt.edu.cn

pressure of CH_4 in the cleat system[4, 5]. An accurate understanding of the pure gas adsorption/desorption characteristics in a specific coal is essential for the design of CBM recovery[6]. Crushed coal in experiments is generally used to measure the adsorption/desorption of pure gas because of remarkable reduction of the experimental time[7, 8].

Some parameters of coal particle size, coal rank, moisture, temperature and shrinkage/swelling that play important role in the adsorption/desorption of gases on/from coal have been analyzed through experimental observation[8, 9]. However, the influence of thermal effect on gas ad/desorption has not been well understood. Crosdale et al., 2008 thought that temperature had insignificant effect on storage capacity of low rank coals through the thermal experiment[10]. While some studies have shown that adsorption capacity decreases significantly with increasing temperature for the high rank coals[11]. Zhou and Lin, 1999 found that when the temperature was increased by 1°C, the adsorption capacity could be reduced about 8%[12]. Obviously, Langmuir gas sorption models can't well match these observation results, because it predicts that the sorption capacity is independent of temperature[6,13]. Even though the Langmuir pressure p_L, it was found that the Langmuir pressure p_L decrease with increasing temperature and vary as a function of rank [10, 14,15].

In this work, the motivation for this study is several-fold to fill the knowledge of adsorption characteristics of equilibrium and thermodynamics. First, the adsorption equilibrium isotherms for pure CH_4 and CO_2 on the coal at 35°C 50°C and 65°C were acquired by static volumetric method. Second, adsorption affinities of CH_4 and CO_2 on different coals and temperatures were analyzed based on SLD-Peng–Robinson (SLD-PR) model. Third, adsorption behavior of pure CH_4 and CO_2 was explained based on adsorption potential and surface free energy.

Adsorption Equilibrium

Many adsorption models have been performed based on the different theoretical foundation, mainly including the mechanisms of monolayer surface adsorption, multilayer surface adsorption and pore filling[6,15]. In this work, the simplied local-density (SLD) adsorption model based on pore filling mechanism is utilized to describe the adsorption behavior of pure gases on a coal. The model envisions that (1) the chemical potential at any point near the adsorbent surface is equal to the bulk-phase chemical potential, and (2) the chemical potential at any point above the surface is the sum of the fluid–fluid and fluid–solid interactions[16], as illustrated in Fig. 1. In other word, the SLD model is used to account for the fluid−fluid and fluid−solid interactions in a slit-shaped pore. For a slit of width L, the equilibrium chemical potential of the fluid, μ, is calculated by contributions from these fluid–fluid and fluid–solid interactions at a position, z, as follows[16]:

$$\mu(z) = \mu_{ff}(z) + \mu_{fs}(z) = \mu_{bulk} \quad (1)$$

where subscripts “ff” and “fs” denote the fluid−fluid and fluid−solid interactions, respectively. The subscript “bulk” refers to the bulk fluid, whose chemical potential can be expressed in terms of fugacity as [17]

$$\mu_{bulk} = \mu_0(T) + RT\ln\left(\frac{f_{bulk}}{f_0}\right) \quad (2)$$

where subscript ‘‘0’’ designates an arbitrary reference state and ‘‘f’’ refers to fugacity.

The chemical potentials from fluid–fluid and fluid–solid interactions are respectively given as[18], respectively.

$$\mu_{\mathrm{ff}}(z) = \mu_0(T) + RT\ln\left[\frac{f_{\mathrm{ff}}(z)}{f_0}\right] \tag{3}$$

$$\mu_{\mathrm{fs}}(z) = N_{\mathrm{a}}\left[\Psi^{\mathrm{fs}}(z) + \Psi^{\mathrm{fs}}(L - z)\right] \tag{4}$$

where $f_{\mathrm{ff}}(z)$ is fluid fugacity at a position z , N_{a} is Avogadro's number, and $\Psi^{\mathrm{fs}}(z)$ and $\Psi^{\mathrm{fs}}(L- z)$ are the fluid−solid interactions for the two surfaces of a slit of length L.

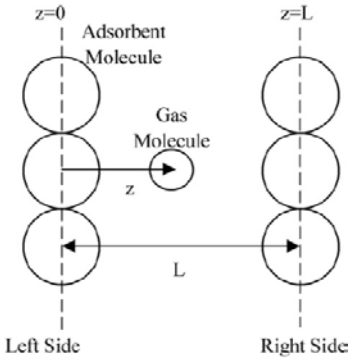

Fig. 1. Schematic of a slit-shaped pore model in the SLD approach[14]

Substituting Eqs. 2-4 into Eq. 1, we can obtain the equilibrium relationship for adsorption within the slit

$$\ln\frac{f_{\mathrm{ff}}(z)}{f_{\mathrm{bulk}}} = -\frac{1}{kT}\left[\Psi^{\mathrm{fs}}(z) + \Psi^{\mathrm{fs}}(L - z)\right] \tag{5}$$

where k is the Boltzmann's constant, and the fluid–solid interaction $\Psi^{\mathrm{fs}}(z)$ can be represented by Lee's partially integrated 10–4 potential[18]

$$\Psi^{\mathrm{fs}}(\mathrm{z}) = 4\pi\rho_{\mathrm{atoms}}\varepsilon_{\mathrm{fs}}\sigma_{\mathrm{fs}}^2\left(\frac{\sigma_{\mathrm{fs}}^{10}}{5(\mathrm{z} + \sigma_{\mathrm{ss}}/2)^{10}} - \frac{1}{2}\sum_{\mathrm{i}=1}^{4}\frac{\sigma_{\mathrm{fs}}^{4}}{(\mathrm{z} + \sigma_{\mathrm{ss}}/2 + (\mathrm{i} - 1)\cdot\sigma_{\mathrm{ss}})^{4}}\right) \tag{6}$$

where $\varepsilon_{\mathrm{fs}}$ is the fluid−solid interaction energy parameter, ρ_{atoms} is the solid atom density. σ_{fs} and σ_{ss} are the fluid−solid molecular diameter and the carbon interplanar distances, respectively. Their relation can be defined as

$$\sigma_{\mathrm{fs}} = \frac{\sigma_{\mathrm{ff}} + \sigma_{\mathrm{ss}}}{2} \tag{7}$$

where σ_{ff} is the molecular diameter.

In terms of bulk fluid density and fugacity, the Peng–Robinson equations of state (PR-EOS) are used to provide [19].

$$\frac{p}{\rho_{\mathrm{bulk}}RT} = \frac{1}{1 - b\rho_{\mathrm{bulk}}} - \frac{a(T)\rho_{\mathrm{bulk}}}{RT\left[1 + (1 - \sqrt{2})b\rho_{\mathrm{bulk}}\right]\left[1 + (1 + \sqrt{2})b\rho_{\mathrm{bulk}}\right]} \tag{8}$$

$$\ln\frac{f_{\mathrm{bulk}}}{p} = \frac{b\rho_{\mathrm{bulk}}}{1 - b\rho_{\mathrm{bulk}}} - \frac{a(T)\rho_{\mathrm{bulk}}}{RT(1 + 2b\rho_{\mathrm{bulk}} - b^2\rho_{\mathrm{bulk}}^2)} - \ln\left(\frac{p}{RT\rho_{\mathrm{bulk}}} - \frac{pb}{RT}\right) - \frac{a(T)}{2\sqrt{2}RTb}\ln\frac{1 + (1 + \sqrt{2})b\rho_{\mathrm{bulk}}}{1 + (1 - \sqrt{2})b\rho_{\mathrm{bulk}}}$$

（9）

where p is the gas pressure within the systerm, and a(T) and b are the energy and co-volume parameters of the adsorbed gas phase, which can be described as:

$$\begin{cases} a(T) = \dfrac{0.457535\alpha(T)R^2T_c^2}{p_c} \\ b = \dfrac{0.077796RT_c}{p_c} \end{cases} \quad (10)$$

where T_c and p_c are the critical gas temperature and pressure, respectively. The term, $\alpha(T)$, can be expressed as [20]

$$\alpha(T) = \exp\left(\left(A + BT_r\right)\left(1 - T_r^{C+D\omega+E\omega}\right)\right) \quad (11)$$

where A, B, C, D, and E are correlation parameters.

For the adsorbing fluid, the fugacity for fluid–fluid interactions is

$$\ln\frac{f_{ff}(z)}{p} = \frac{b\rho(z)}{1-b\rho(z)} - \frac{a_{ads}(z)\rho(z)}{RT\left(1+2b\rho(z)-b^2\rho^2(z)\right)} - \ln\left(\frac{p}{RT\rho(z)} - \frac{pb}{RT}\right) - \frac{a_{ads}(z)}{2\sqrt{2}RTb}\ln\frac{1+\left(1+\sqrt{2}\right)b\rho(z)}{1+\left(1-\sqrt{2}\right)b\rho(z)} \quad (12)$$

where $a_{ads}(z)$ depends on the ratio of slit length L to the molecular σ_{ff}.

The excess adsorption can be expressed as [16]:

$$n^{ex} = \frac{A_s}{2}\int_{\frac{3}{8}\sigma_{ff}}^{L-\frac{3}{8}\sigma_{ff}}(\rho(z)-\rho_{bulk})dz \quad (13)$$

where A_s is the surface area per unit mass of adsorbent.

Materials and experimental procedure

One typical coal obtained from Anhui province was used in this study. The coal sample was preserved in sealed plastic bags with helium preventing oxidation. The experimental sample was pulverized into particles with diameter between 180 and 250 μm. Because moisture can have a great effect on adsorption, all samples are dried in a vacuum oven at 80°C for over 36 h to remove the moisture before adsorption[21]. Adsorption equilibrium isotherms of CH_4 and CO_2 were performed at different temperatures of 35°C, 50°C and 65°C using a static volumetric instrument (as shown in [22]).

Results and discussion

Adsorption Equilibrium Isotherms

Equilibrium isotherm data of pure CH_4 and CO_2 at 35°C, 50°C and 65°C on coal were well matched using SLD model, as shown in Fig. 3 a and b. The parameters of SLD model for adsorption of CH_4 and CO_2 can be found in table 1. As can been seen from Fig. 2 a and b, the higher temperature corresponds to the smaller adsorption quantity, while the larger gas pressure corresponds to the larger adsorption quantity. It is because the increase of temperature and the decrease of gas pressure will cause more thermal energy or lower constraint force for adsorbate, resulting in many gas molecules slit-shaped pore escaping the adsorbent surface[23]. For example, the highest excess

adsorption quantity of CH_4 and CO_2 occurs at 35°C among experimental temperatures at the same gas pressure level. When the gas pressures are 6.294 and 4.333MP, respectively, corresponding to the highest excess adsorption quantity of CH_4 and CO_2 are 1.812 and 2.169 mmol/g, respectively.

Table 1. SLD regression parameters for gas adsorption

Gases	T_c(K)	p_c(MPa)	σ_{ff}(nm)	A_s(m^2/g)	L(nm)	σ_{fs}(nm)	σ_{ss}(nm)	ε_{ff}/k(K)		
								35℃	50℃	65℃
CH_4	190.56	4.599	0.3758	138	1.02	0.38	0.34	129	90	69
CO_2	304.13	7.377	0.3941					165	105	91

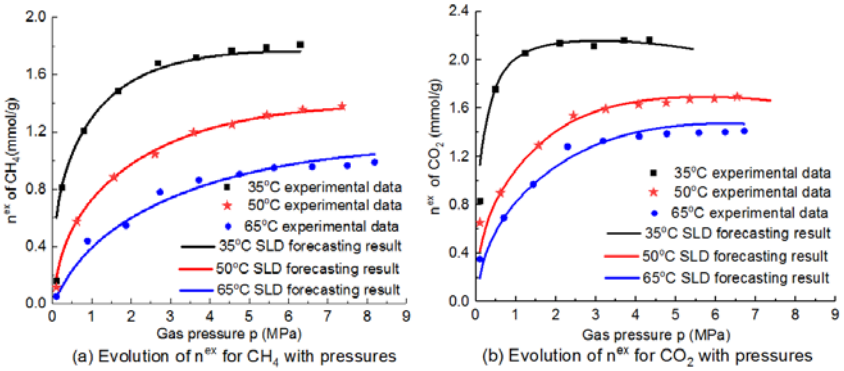

Fig.2 Experimental data and SLD fitting results under different temperatures

Adsorption potential

The concept of adsorption potential reflects the variation of Gibbs free energy under the adsorption of 1 mol mass. It can be described as[24]

$$\varepsilon = \int_{p_i}^{p_0} RT\mathrm{d}(\ln p) = RT\ln\frac{p_0}{p_i} \qquad (14)$$

where ε is the adsorption potential, J/mol; p_0 is the saturation vapor pressure of the adsorbate at temperature *T*, MPa; p_i is the equilibrium pressure of ideal gas under a constant temperature, MPa.

An empirical formula of the saturation vapor pressure in the adsorbate under supercritical conditions was proposed [25]

$$p_0 = p_c\left(\frac{T}{T_c}\right)^2 \qquad (15)$$

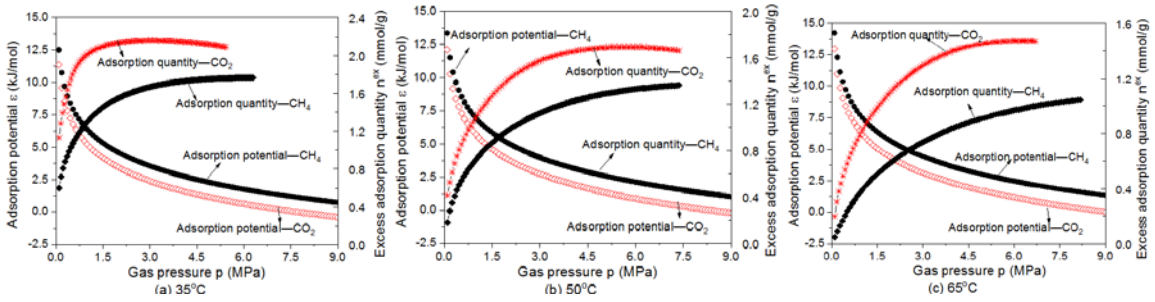

Fig. 3 Comparison of adsorption potential and adsorption quantity under different temperatures

Fig. 3 a-c shows the comparison of adsorption potential and adsorption quantity for CH_4 and CO_2 under different temperatures. There is the same law of changes of adsorption potential and

adsorption quantity in these three pictures. It can be concluded from every picture that (i) the adsorption potential decreases with the increase of gas pressure. that is, the greater the adsorption potential is, the smaller adsorption capacity of the gas is. (ii) the adsorption potential and adsorption quantity for CO_2 are all larger than CH_4 under the same conditions of adsorption pressure and temperature. Thus, the greater the adsorption potential for one gas is, the stronger adsorption capacity of the gas is.

Surface free energy

According to surface chemistry theory, Surface tension reduction induced by gas adsorption in coal can be described as[24]

$$-\mathrm{d}\sigma = \frac{n^{\mathrm{ex}}}{A_s} RT\mathrm{d}(\ln p) \tag{16}$$

where σ is the surface tension, J/m^2 .

In order to get the integral result of Eq. 16, we take a modified Langmuir or Freundlich equation to match the results based on SLD models at different temperatures. The modified Langmuir or Freundlich equation can be expressed as

$$n^{\mathrm{ex}} = \frac{a_1 b_1 p^{1-c_1}}{1+b_1 p^{1-c_1}} \tag{17-a}$$

$$n^{\mathrm{ex}} = a_1 p^{b_1 p^{-c_1}} \tag{17-b}$$

where a_1, b_1 and c_1 are fitting constants. As shown in table 2, we found that the modified Langmuir equation can well match the curves of SLD model when adsorption medium is CH_4. However, when the adsorption medium is CO_2, the modified Freundlich equation is better.

Table 2. SLD regression parameters for gas adsorption

Fitting equation of SLD model for CH_4						Fitting equation of SLD model for CO_2					
Equation	Temperatures	Parameters			R^2	Equation	Temperatures	Parameters			R^2
		a_1	b_1	c_1				a_1	b_1	c_1	
$n^{\mathrm{ex}} = \frac{abp^{1-c}}{1+bp^{1-c}}$	35 °C	2.07	9.22e-5	0.29	0.99	$n^{\mathrm{ex}} = ap^{\mathrm{b}p^{-c}}$	35 °C	1.33e-5	2.07	0.06	0.93
	50 °C	1.78	1.09e-5	0.20	1.0		50 °C	2.19	-178.58	0.6	0.98
	65 °C	1.41	5.6e-7	0.03	1.0		65 °C	2.29	-199.91	0.54	0.99

The variations of surface free energy of coals $\Delta\gamma$ due to gas adsorption based on the two modified fitting equations can be derived, respectively

$$\Delta\gamma = \frac{a_1 RT}{A_s(1-c_1)} \ln(1 + b_1 p^{1-c_1}) \tag{18-a}$$

$$\Delta\gamma = \frac{a_1 RT}{A_s} \int p^{b_1 p^{-c_1}-1} \mathrm{d}p \tag{18-b}$$

Further, the changes of surface free energy $\Delta\gamma_p$ at a given pressure can be obtained, respectively

$$\Delta\gamma_p = \frac{a_1 b_1 RT p^{-c_1}}{A_s(1+b_1 p^{1-c_1})} \tag{19-a}$$

$$\Delta\gamma_p = \frac{a_1 RT}{A_s} p^{b_1 p^{-c_1}-1} \quad (19\text{-b})$$

As we know, any object tends to decrease its surface free energy for a more stable state. The surface free energy of coals will decrease with gas adsorption, which reflects gas adsorption capacity. That is, the greater the reduction of surface free energy is, the larger the gas adsorption capacity is. Fig. 4 illustrates the variation of surface free energy $\Delta\gamma$ and its reduction rate $\Delta\gamma_p$ at a given pressure under different temperatures. It can be seen from Fig. 4(I) that the variation of surface free energy $\Delta\gamma$ increases with the increase of gas pressure under the same temperature, decreases with the increase of temperature under the same gas pressure. The variation of surface free energy $\Delta\gamma$ for CH_4 is smaller than CO_2 under the same gas pressure and temperature. Compared with the variation of surface free energy$\Delta\gamma$ in Fig. 4(I), the reduction rate of surface free energy $\Delta\gamma_p$ exhibits an inverse relationship as shown in Fig. 4(II). That is, the reduction rate of surface free energy $\Delta\gamma_p$ decreases with the increase of gas pressure under the same temperature. However, the reduction rate of surface free energy $\Delta\gamma_p$ decreases also with the increase of temperature under the same gas pressure.

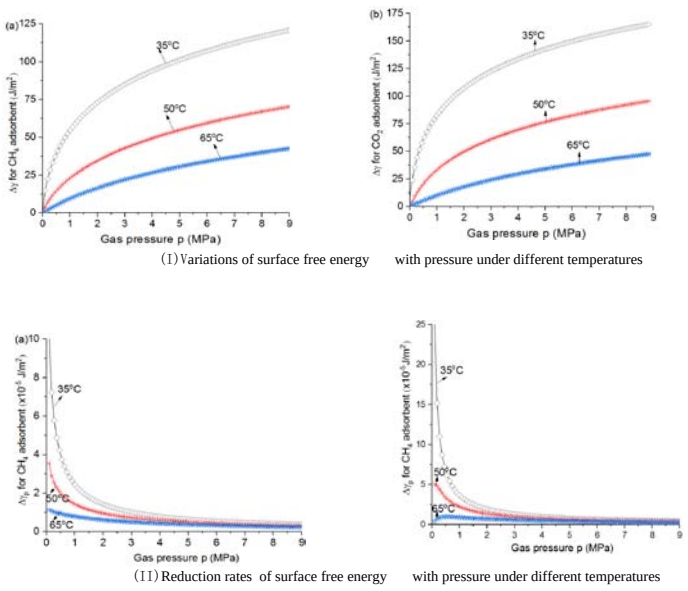

Fig. 4 Variations of surface free energy $\Delta\gamma$ and its reduction rate $\Delta\gamma_p$ at a given pressures under different temperatures

Conclusion

In this study, adsorption equilibrium isotherms of CH_4 and CO_2 on the same coal under different pressures and temperatures were analyzed based on SLD-PR model. The adsorption equilibrium curves of the same coal are different because of adsorbents. When the adsorbent is CH_4, the SLD adsorption model can be well represented by the modified Langmuir equation. However, it is well matched by the modified Freundlich equation as the adsorbent is CO_2. Based on the analysis of roles of temperature, pressure, adsorption potential and surface free energy on gas adsorption capacity, the main conclusions can be drawn: The higher temperature corresponds to the smaller excess adsorption quantity of gas, while the larger gas pressure corresponds to the larger excess adsorption

quantity. The larger the gas adsorption capacity is, the adsorption potential and the reduction of surface free energy are, and the smaller the reduction rate of surface free energy is.

Acknowledgement

This work was supported by the National Key Research and Development Program of China (2018YFC0808100), the National Science Foundation of China (51604269), Postdoctoral Science Foundation funded project of China (2017M621877), Open Projects of State Key Laboratory of Coal Resources and Safe Mining (SKLCRSM16KFD06), Research Center of Coal Resources Safe Mining and Clean Utilization in Liaoning (LNTU16KF12), and Hebei State Key Laboratory of Mine Disaster Prevention (KJZH2017K11).

Nomenclature

L—a slit of width,[nm]
ρ_{atoms}—the number of carbon plane atoms per unit area,[atoms/Å^2]
p_c—critical pressure,[MPa]
k —Boltzmann's constant, [J/K]
σ—surface tension, [J/m^2]
A_s—surface area,[nm^2/g]
z—location parameter,[nm]
n^{ex}—excess adsorption,[mmol/g]
T_c—critical temperature,[K]

References

[1] Liu, J., *et al.,* Interactions of Multiple Processes during CBM Extraction: a Critical Review. *International Journal of Coal Geology,* 87 (2011), 3-4, pp. 175-189.
[2] Xia, T. Q., Role of Thermodynamic Effect on Coal-gas Interactions during Underground Pre- and Post-mining Coal Seams in the Environmental Geology. *Journal of Environmental Geology,* 1(2017), Oct, 16, pp. 7-8.
[3] Xia, T. Q., *et al.,* Fluid Flow in Unconventional Gas Reservoirs. *Geofluids*, 2018, pp. 1-2. https://doi.org/10.1155/2018/2178582
[4] Zhou F. D., *et al.,* Injecting Pure N_2 and CO_2 to Coal for Enhanced Coalbed Methane Experimental Observations and Numerical Simulation. *International Journal of Coal Geology,* 116 (2013), pp. 53-62.
[5] Puri, R., *et al.,* Enhanced Coalbed Methane Recovery. *The 65th Annual Technical Conference and Exhibition of the Society of Petroleum Engineers,* New Orieans, LA, Oct 5-8, 2019.
[6] Perera, M. S. A., *et al.,* Estimation of Gas Adsorption Capacity in Coal: A Review and an Analytical Study, *International Journal of Coal Preparation and Utilization,* 32(2012), 1, pp. 25-55.
[7] Sudibandriyo, M., *et al.,* Adsorption of Methane, Nitrogen, Carbon Dioxide and Their Binary Mixtures on Dry Activated Carbon at 318.2 K and Pressures to 13.6 MPa. *Langmuir,* 19(2003), 13, pp. 5323-5331
[8] Hall, F., *et al.,* Adsorption of Pure Methane, Nitrogen, and Carbon Dioxide and Their Binary Mixtures on Wet Fruitland Coal. *SPE Paper 29194, Charleston,* SC; November,1994.
[9] Zhang, D. F., *et al.,* Supercritical Pure Methane and CO_2 Adsorption on Various Rank Coals of

China: Experiments and Modeling. *Energy & Fuels*, 25(2011), 4, pp. 1891–1899.
[10] Crosdale, P. J., *et al.*, Influence of Moisture Content and Temperature on Methane Adsorption Isotherm Analysis for Coals from a Low-rank, Biogenically-sourced Gas Reservoir. *International Journal of Coal Geology*, 76(2008), 1-2, pp. 166-174.
[11] Krooss, B. M., *et al.*, High-pressure Methane and Carbon Dioxide Adsorption on Dry and Moisture-equilibrated Pennsylvanian Coals. *International Journal of Coal Geology*, 51(2002), 2, pp. 69-91
[12] Zhou, S. N., *et al.*, *Coalbed Methane Occurrence and Flow Theory*. Beijing: Coal Industry Press, 1999.
[13] Charoensuppanimit, P., *et al.*, Modeling the Temperature Dependence of Supercritical Gas Adsorption on Activated Carbons, Coals and Shales. *International Journal of Coal Geology*, 138(2015), pp. 113–126.
[14] Lama, R. D., *et al.*, Management of Outburst in Underground Coal Mines. *International Journal of Coal Geology*, 35(1998), 1-4, pp.83-115.
[15] Rexer, T. F., *et al.*, High-pressure Methane Adsorption and Characterization of Pores in Posidonia Shales and Isolated Kerogens. *Energy & Fuels*, 28(2014), 5, pp.2886–2901.
[16] Meysam, H., *et al.*, Simplified Local Density Model for Adsorption of Pure Gases on Activated Carbon Using Sutherland and Kihara Potentials. *Microporous and Mesoporous Materials*, 136(2010), 1-3, pp. 1–9.
[17] Sayeed, A. M., *et al.*, High-Pressure Adsorption of Pure Gases on Coals and Activated Carbon: Measurements and Modeling. *Energy & Fuels*, 26(2012), 1, pp. 536−548.
[18] Lee, L. L., Molecular Thermodynamics of Nonideal Fluids; Butterworth: Stoneham, MA, 1988.
[19] Fitzgerald, J. E., *et al.*, Modeling High-Pressure Adsorption of Gas Mixtures on Activated Carbon and Coal Using a Simplified Local-Density Model. *Langmuir*, 22(2006), 23, pp. 9610−9618.
[20] Gasem, K. A. M., *et al.*, A Modified Temperature Dependence for the Peng−Robinson Equation of State. *Fluid Phase Equilibria*, 181 (2001), 1-2, pp. 113−125.
[21] Robert, L., *et al.*, Adsorption Characteristics of Coals Pyrolyzed at Slow Heating Rates. *Energy & Fuels*, 31(2017), 2, pp. 1803−1810.
[22] Zhao, W., *et al.*, Modeling and Experiments for Transient Diffusion Coefficients in the Desorption of Methane Through Coal Powders. *International Journal of Heat and Mass Transfer*, 110(2017), Jul., pp. 845-854.
[23] Meng, Z. P., *et al.*, Adsorption Capacity, Adsorption Potential and Surface Free Energy of Different Structure High Rank Coals. *Journal of Petroleum Science and Engineering*, 146(2016), Oct., pp. 856–865.
[24] Ramirez-Pastor, A. J., *et al.*, Differential Heat of Adsorption in the Presence of an Order-disorder Phase Transition. *Physica A*, 283 (2000), 1-2, pp. 198–203.
[25] Jian, K., *et al.*, The Surface Energy of Methane Adsorption of Tectonic Coal. *Coal Geology & Exploration*, 42 (2014), 1, pp. 31–39.

Paper submitted: June 5, 2018
Paper revised: September 10, 2018
Paper accepted: November 10, 2018